J. exp. Biol. **140**, 137–160 (1988)
Printed in Great Britain © *The Company of Biologists Limited 1988*

THE IMPORTANCE OF TORSION IN THE DESIGN OF INSECT WINGS

BY A. ROLAND ENNOS*

Department of Biological Sciences, Hatherly Laboratories, University of Exeter, Prince of Wales Road, Exeter EX4 4PS

Accepted 5 May 1988

Summary

A model insect wing is described in which spars of corrugated membrane which incorporate stiffening veins branch serially from a V-section leading edge spar. The mechanical behaviour of this model is analysed.

The open, corrugated spars possess great resistance to bending, but are compliant in torsion. Torsion of the leading edge spar will result in torsion and relative movement of the rear spars. As a result camber will automatically be set up in the wing as it twists.

Aerodynamic forces produced during the wing strokes will result in torsion and camber of the wing which should improve its aerodynamic efficiency.

The effects of varying parameters of the wing model are examined. For given wing torsion, higher camber is given by spars branching from the leading edge at a lower angle, by spars which curve posteriorly, and by spars which diverge from each other.

Wings of three species of flies were each subjected to two series of mechanical tests. Application of a force behind the torsional axis caused the wings to twist and to develop camber. Immobilizing basal regions of the leading edge greatly reduced compliance to torsion and camber, as predicted by the theoretical model. Aerodynamic forces produced during a half-stroke are sufficient to produce observed values of torsion and camber, and to maintain changes in pitch caused by inertial effects at stroke reversal.

Introduction

The structural role of corrugation in the wings of insects was noted by Hertel (1966) who likened the arrangement of longitudinal veins in dragonfly wings to the cross-sections of man-made girders. The idea was extended by Rees (1975*a*) to other insects and he calculated that the use of corrugation greatly increased both the stiffness and strength of insect wings. Rees (1975*b*) and Newman *et al.* (1977) further demonstrated that at the Reynolds numbers characteristic of insect flight a corrugated wing made a good aerofoil. Newman & Wootton (1986) have recently shown that in such corrugations the membrane itself may have a structural role,

* Present address: Department of Biological Science, University of York, Heslington, York, YO1 5DD.

Key words: insect, wing, torsion, camber, flight.

further stiffening the wing by means of a 'stressed skin' effect. They also discuss modes of failure and suggest that the use of the corrugated structure allows the wing to deform without damage when it is subjected to impact loading. This would absorb the kinetic energy of the wing and protect the wing articulation from excessive shocks.

The arguments so far presented are based on the premise that insect wings are designed for maximum stiffness and minimum weight. This is, however, inadequate to explain the arrangement of individual corrugations in wings. It was necessary to examine the detailed kinematics and instantaneous deformations of the wings in flight and relate them to the wing structure as Wootton (1981) recommended. The results of my study of the kinematics of flies in free flight will be published (A. R. Ennos, in preparation).

Kinematics and wing deformations

High-speed cinematography has given us a wealth of information on the kinematics of insect flight. Most of the insects so far filmed produce useful aerodynamic forces during both the downstroke and upstroke in both normal hovering and forward flight (Weis-Fogh, 1973; Ellington, 1984*a*,*b*; Dudley, 1987), reversing the upper and lower surfaces by rotating the wings about their longitudinal axis by over 90° between half-strokes (Fig. 1). To optimize force production the main wing area should also undergo two forms of deformation. (a) The wing should twist nose down towards the tip during each stroke to assume a propeller-like shape. As a result each wing section will strike the oncoming air at a similar angle of attack, despite the increase in flapping velocity towards the tip,

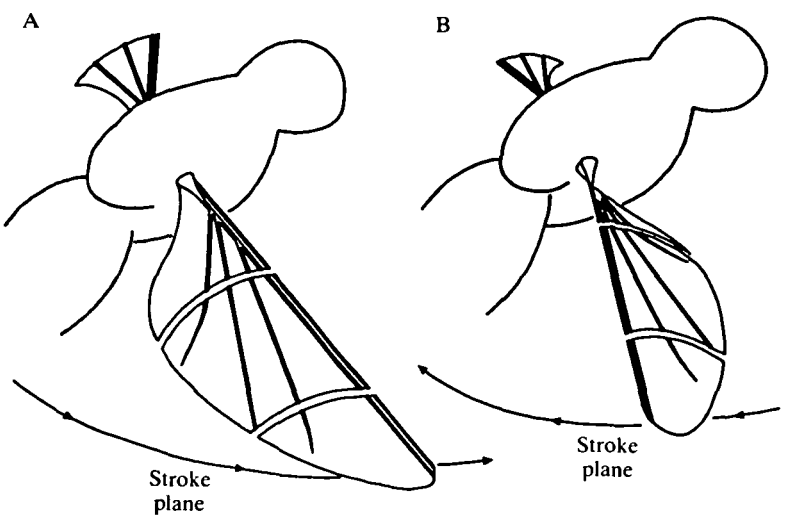

Fig. 1. Reversal of camber and torsion. Wings of a typical insect during (A) the downstroke; and (B) the upstroke. Two chordwise sections are shown in the near wing. The camber and torsion of the wing are of opposite signs during the two strokes. (After Wootton, 1981.)

and can produce high lift and low drag. (b) The wing should be positively cambered to produce high lift and a high lift to drag ratio. In tests both Vogel (1967) and Dudley (1987) have found that cambered wings can produce higher lift than flat ones, and often have a higher maximum lift to drag ratio.

Both the twist and the camber must be reversed between half-strokes (Fig. 1). There are no muscles in the main wing area of insects to bring about these shape changes, and in many insects direct muscles could not operate at the high frequencies required. Shape changes must therefore be brought about automatically by the forces which occur during the wingbeat.

The centre of torsion of insect wings (as defined for dragonfly wings by Norberg, 1972) tends to be very close to the leading edge and therefore anterior to the aerodynamic centre of pressure. Aerodynamic forces will therefore tend to twist the wing in the manner required. I have shown (Ennos, 1988) that the inertia of the wing can cause it to rotate at stroke reversal to cause the necessary changes in pitch.

In the main section of this paper the torsional behaviour of simplified wing structures is analysed, to investigate how such shape changes can be brought about by forces that are incapable of significantly bending the wing. It will be shown that many aspects of wing structure and venation can be explained by considering the effects of torsion. Mechanical tests that were carried out on the wings of three species of flies to test the local validity of the structural model are then described.

The torsional rigidity of structures

Gordon (1978) gives a good introduction to the two major methods of resisting torsion.

The torsion box

The most efficient way of resisting torsion is by the use of a *closed* torsion box such as the monocoque wing of a modern aircraft. The polar second moment of area K of a box with wall thickness t, section perimeter U, enclosing an area A is given by the formula:

$$K = A^2t/U \, . \tag{1}$$

If the box is split along its length or one wall removed, however, the torsional stiffness falls dramatically to the new value:

$$K = Ut^3 \, . \tag{2}$$

Closed boxes are far stiffer in torsion than open ones.

Differential bending stiffness

If a structure such as a wing is supported by two more or less parallel spars, firmly cantilevered to a common base, twisting the wingtip will necessarily involve bending the spars. Their resistance to bending will confer a resistance to torsion known as differential bending stiffness.

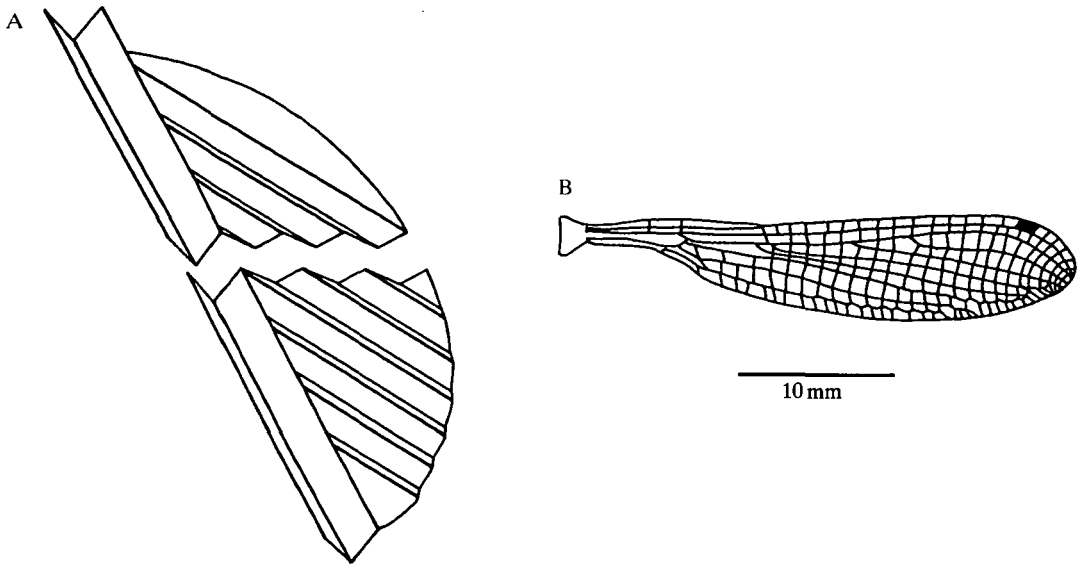

Fig. 2. (A) The basic model of the wing. Corrugated spars diverge at an equal angle from the leading edge spar. (B) The wing of the damselfly *Pyrrhosoma nymphula* has a similar structure.

The basic wing model

The basic model insect wing is shown in Fig. 2A. The leading edge is supported by a beam of membrane of V-shaped cross-section, reinforced by three longitudinal veins, one at each peak of the V and the other at the bottom of the trough. This condition is commonly seen in many insect groups (Wootton, 1981). The rear wing area is composed of slightly shallower membrane corrugations, also reinforced by veins at the peaks and troughs, forming cantilevered beams or spars which branch off from the leading edge spar at an angle Θ. The wing which results is very similar to those of the narrow-winged damselflies (Fig. 2B).

Behaviour in torsion

As previous authors have noted, these corrugated beams or spars are very rigid in bending. Each separate corrugation, however (including the leading edge spar), has an open V cross-section and as a result has a very low torsional rigidity. There will be high differential bending stiffness between the leading edge and each rear spar, but not *between* the rear spars, since each has a base on a separate point of the leading edge.

Aerodynamic forces produced in flight will not significantly bend the spars, but as these forces act behind the leading edge they may twist it fairly easily. The rear spars will be angled up or down relative to each other as their bases at the leading edge are rotated. Each of the spars will thus have to twist along its length and the shape of chordwise wing sections will change.

The degree of torsion caused in the rear spars, and the chordwise change in

shape of the wing membrane caused by twisting the leading edge by an angle Ψ per unit length are analysed below.

Torsion of rear spars

Two adjacent spars are shown in Fig. 3A separated along the leading edge by a distance x and diverging from it at an angle Θ. After pronation of the leading edge the base of the outer spar will have been rotated by an angle ψ relative to the inner one where

$$\psi = \Psi x \tag{3}$$

and the outer spar will be raised relative to the inner one. A point on the outer spar a perpendicular distance y behind the leading edge will be raised to a height, h, where

$$h = \Psi xy\,. \tag{4}$$

The membrane joining the two spars must therefore slope, and the spars themselves must twist along their length to allow this. Clearly the membrane joining the spars will give an upper limit to h. The angle of torsion ψ_r at this point is

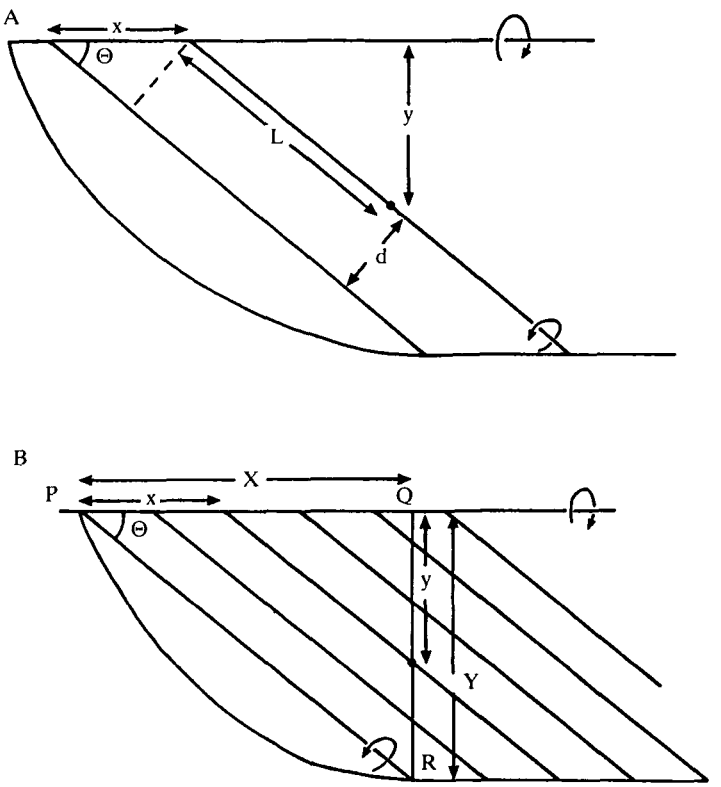

Fig. 3. Plans of spars branching from the leading edge, for use on conjunction with text calculations of: (A) torsion of the rear spars when the leading edge is twisted; (B) out-of-plane displacement of rear spars when the leading edge is twisted. See text for details of notation.

found using the small angle approximation to be the height of the outer spar, h, divided by the perpendicular distance between the spars, d, where $d = x\sin\Theta$.

$$\psi_r = h/d = \Psi xy/x\sin\Theta$$
$$= \Psi y/\sin\Theta \,. \tag{5}$$

The torsion per unit length Ψ_r of the outer spar can be found by dividing this angle by the length of the spar from its base, L, at this point. Since $L = y/\sin\Theta$, then

$$\Psi_r = \psi_r/L = \Psi y\sin\Theta/y\sin\Theta$$
$$= \Psi \,. \tag{6}$$

Each spar will therefore twist by the same angle per unit length as the leading edge but in the opposite direction, so that if the leading edge is pronated, each spar will supinate and *vice versa*.

Change in cross-sectional shape

The wing is shown again in Fig. 3B. We will examine the upward displacement of the membrane along the chordwise section QR which has a length Y. As we have seen, the spar which crosses the section a distance y behind the leading edge and which branches off a distance x from point P, has a height h at the section given by equation 4:

$$h = \Psi xy \,.$$

A spar which branches from the leading edge near its base will cross the chordwise section near the trailing edge. x and y are therefore related by the geometrical relationship:

$$y = (X - x)\tan\Theta \,, \tag{7}$$

where X is the length PQ. As $X\tan\Theta = Y$ this equation can be manipulated to give an expression for x:

$$y = Y - x\tan\Theta \,,$$
$$x = (Y - y)/\tan\Theta \,. \tag{8}$$

Substituting this expression for x into equation 4 gives:

$$h = \Psi y(Y - y)/\tan\Theta$$
$$= (yY - y^2)\Psi/\tan\Theta \,. \tag{9}$$

The membrane will arch up in an inverted parabola (Fig. 5C). The maximum displacement will occur when the differential of displacement h from the chord with respect to the distance y along the section $\partial h/\partial y = 0$, that is when

$$\partial h/\partial y = (Y - 2y)\Psi/\tan\Theta = 0 \,,$$
$$Y - 2y = 0 \,,$$
$$y = Y/2 \,. \tag{10}$$

The maximum displacement occurs at mid-section where h_{max} will be:

$$h_{max} = \Psi Y^2/4\tan\Theta \, . \tag{11}$$

The camber of a wing section is defined as the maximum displacement from the wing chord divided by the length of the chord, Y. In this case the camber produced is h_{max}/Y.

$$\text{Camber} = h_{max}/Y = \Psi Y^2/4Y\tan\Theta$$

$$= \Psi Y/4\tan\Theta \, . \tag{12}$$

If the leading edge is twisted the wing will *automatically* camber symmetrically about the mid chord. The camber is proportional to the torsion of the leading edge and is reversed when torsion is reversed.

This effect is perhaps most clearly demonstrated by means of a simple mechanical model (Fig. 4A), consisting of an open section beam (such as a piece of electrical trunking) to which spars are glued, branching off at equal angles. Twisting the open leading edge beam will set up camber (Fig. 4B) which may be visualized by glueing tape along wing sections.

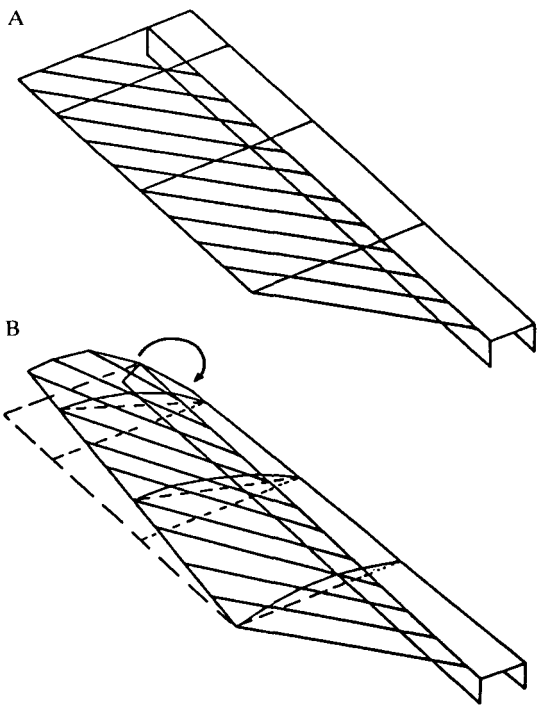

Fig. 4. A perspective view of the mechanical model of the wing. (A) Leading edge untwisted. (B) Leading edge twisted. Outer spars move upwards relative to the inner spars. The wing twists along its length and symmetrical camber is produced. Chordwise sections are visualized with tape.

Behaviour of the complete structure

We have seen that if the leading edge is twisted the rear spars will move up and down relative to each other, twisting in the opposite direction and setting up camber.

If a wing on the downstroke is subjected to aerodynamic forces from below centred behind the centre of torsion, the leading edge will pronate. The wing will be twisted nose down along its length and develop positive camber, and these will both increase its aerodynamic efficiency. The opposite twist and camber are developed on the upstroke.

Given realistic values for wing shape and the branching angle of the spars, the amount of camber produced in the wing for a given change in pitch along its length can be calculated. Take a wing, for instance, of aspect ratio 4 (four times as long as it is broad), chord length Y and wing length 4Y, and with spars branching off at an angle Θ, where $\tan\Theta$ is 0·5 (Fig. 5). If the leading edge is twisted at its tip by an angle ψ of 0·5 rad, its torsion per unit length Ψ is $\psi/4Y$ or $1/8Y$. The camber set up in the wing (from equation 12) is $Y(1/8Y)/4 \times 0{\cdot}5 = 1/16$.

The angle of pitch at the wing tip is set by the spar which reaches the trailing edge at the wing tip. This spar branches from the leading edge a distance 2Y from the base (see Fig. 5), so the change in pitch at the wing tip is only $\Psi \times 2Y$ which

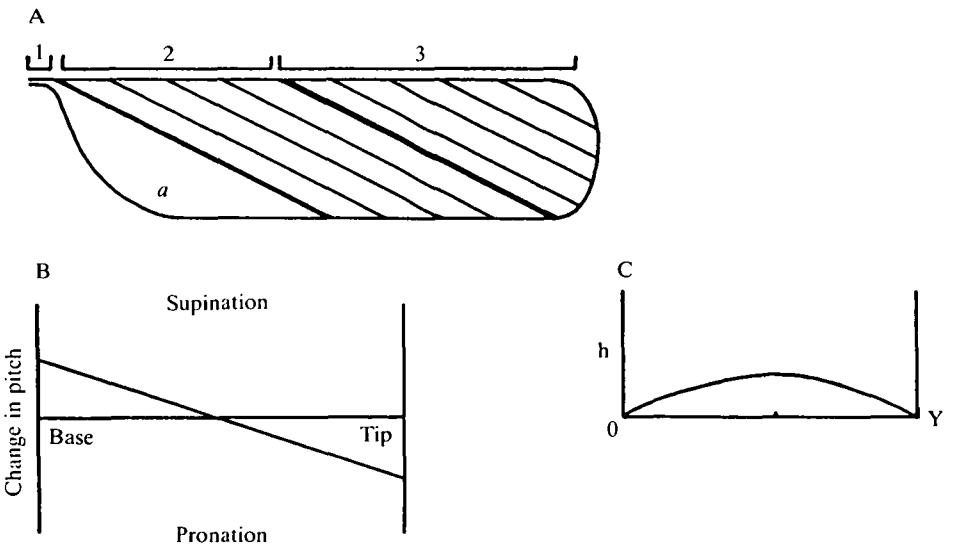

Fig. 5. A wing with length 4Y, chord Y and with parallel spars branching with $\tan\Theta = 0{\cdot}5$. Spars branching at the zone boundaries are drawn thicker than the rest. Pronating the leading edge causes pitch changes along the wing (B). At the point where the first spar to branch reaches the trailing edge (in this case 2Y from the base) there is no pitch change. Inboard of this (in the region *a*) the wing actually supinates. The horizontal line in B is the pitch before torsion. (C) A chordwise wing section 2Y from the base. The wing arches up into symmetrical camber. The horizontal line is the chord of the wing at rest.

equals 0·25 rad. Changing the pitch of the wing tip by only around 15° will produce marked camber of the wing.

The spar which branches from the leading edge at its base reaches the trailing edge a distance 2Y along the wing. The angle of attack at this point will be unaffected by leading edge torsion. Inboard of this, the area *a* is controlled by the innermost spar, which twists in the opposite direction from the leading edge. This inner area will therefore move in the opposite direction from the outer wing: if the pitch of the outer wing is reduced, that of the inner wing will be increased and *vice versa*. Pitch and camber changes are shown graphically in Fig. 5B,C, respectively.

Most wings have a short wing root region, before the first rear spar branches off the leading edge. Torsion of this region will cause pitch changes of the entire wing, but will not affect its shape, since the relative orientation of the rear spars will be unchanged.

Functionally, the leading edge may therefore be divided into three zones (marked on Fig. 5). Zone 1: in the wing root region torsion will cause the same change in wing pitch along the entire wing, but will not affect wing shape. Zone 2: in the region between the branching of the first spar and that of the spar reaching the trailing edge at the wing tip, torsion will change the relative orientation of the rear spars. The angle of pitch will be progressively altered along the wing and camber will be created in the main wing region. Zone 3: no spars branching from this zone reach the trailing edge, so torsion of this zone cannot effect changes in wing pitch, but may only cause camber in anterior distal areas of the wing.

Immobilization of these regions will therefore have different effects on the mechanical properties of the wing. Immobilizing zone 1 will reduce only the torsional compliance of the wing, whereas immobilizing zone 2 should reduce the compliance both to torsion and to camber. Immobilizing zone 3 should affect only camber production.

Modifications of the basic model

Effect of varying the spar angle Θ

It can be seen from equation 12 that the camber produced by a given rotation of the leading edge is inversely proportional to $\tan\Theta$. No camber would be produced if the spars were perpendicular to the leading edge, and low values of Θ give high camber. A lower limit is set to Θ, however, by the need to support the trailing edge of the wing.

Effect of curvature of the rear spars

Instead of being straight, in many insects the rear spars curve gently backwards. If the leading edge is twisted the resulting torsion of the spars will cause their distal ends to move out of their plane of rest, just as rotating a curved rod causes its far end to move. In Fig. 6, for instance, pronation of the leading edge has resulted in supination of the rear spars and, as a result, the distal ends of the spars curve downwards. This will alter the response of the wing to torsion in two ways.

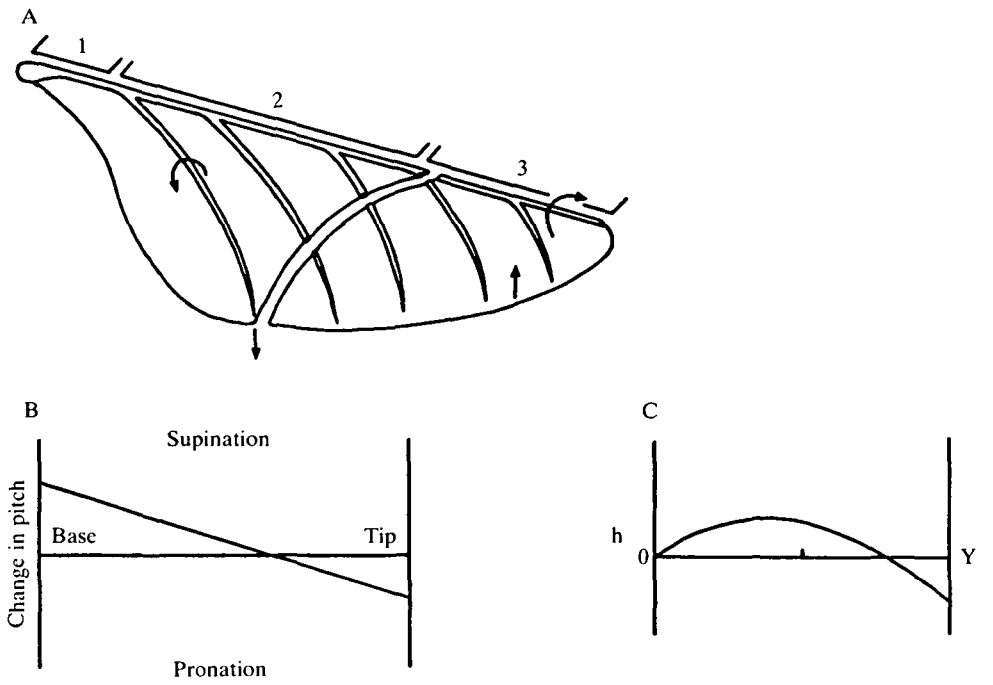

Fig. 6. (A) Wing with curved spars, showing the leading edge zones. Pronation of the leading edge causes the rear spars to supinate and so curve downwards. As a result, the end of the basal rear spar actually *falls* (see diagram: local displacements are shown by the small arrows) and the graph of pitch against distance along the wing (B) is shifted upwards. The chordwise section (C) through the wing at the tip of the basal spar shows the increase in pitch and an increased camber.

(i) Since each spar curves out of the plane, this causes extra camber to be set up for given torsion of the leading edge. (ii) The ends of the spars move in the opposite direction from the applied force. The wing section at the end of the basal spar (Fig. 6B) will therefore supinate if the leading edge is pronated (just as the inner area *a* does in the basic model). This effect was noted by Newman (1982) during his manipulations of the wings of dragonflies. The graph of pitch change against distance from the wing base (Fig. 6B) will be shifted.

The magnitude of these effects will vary with the exact shape of the spars.

Effect of spar divergence

The rear spars of many insect wings are not parallel to each other. Instead, the spars emerge close together from near the base of the wing and diverge rapidly (Fig. 7A). Torsion of the leading edge which affects the angle of attack (zones 1 and 2) is thereby limited to a short region of the wing near the base. For a given torsion of the leading edge, therefore, the change in pitch along the wing will be greatly reduced (Fig. 7B), so more camber will be produced for a given spanwise change in wing pitch.

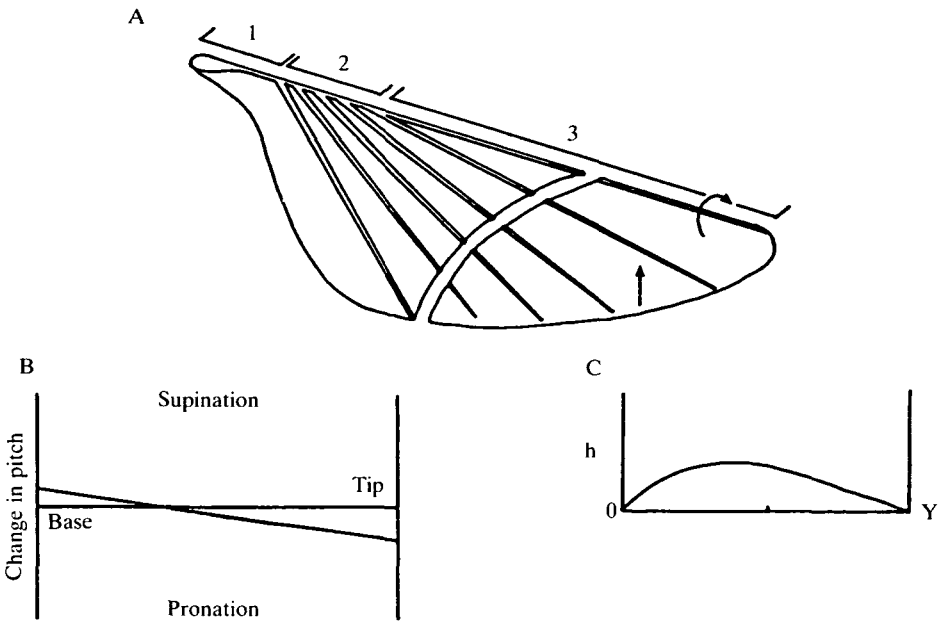

Fig. 7. (A) Wing with diverging spars showing the leading edge zones. Pronation of a shorter region of the leading edge affects the pitch angle (zone 2 is short), so the change in pitch along the wing is reduced (B). The chordwise section (C) at the tip of the basal spar develops camber centred nearer the leading edge.

Spars which branch from the leading edge at equal intervals will cross a chordwise wing section closer together near the front of the chord. The section therefore will have a higher curvature near the leading edge and the centre of camber will be brought forward in front of the mid-chord (Fig. 7C), producing a better aerofoil shape.

Cross veins

Longitudinal spars do not constitute the entire venation pattern of insect wings. Almost all insects possess 'cross veins' that link adjacent longitudinal veins. The effect of twisting the leading edge of a wing is to cause curvature of the wing surface in all directions save those parallel to the spars. To allow camber to be formed, therefore, the cross veins must be flexible and more easily bent than the longitudinal spars. Cross veins do not form a corrugated pattern and so their resistance to bending is far less. They also tend to be thinner than longitudinal veins and may possess specially weakened regions (Wootton, 1981; Newman, 1982). In the main wing region their function may be mainly to maintain the wing planform by preventing the membrane between the spars from folding up.

Experimental tests of the torsion model

The torsional model clearly seems to be a good representation of the wings of

such insects as the members of the Odonata and Ephemeroptera, but the wings of Diptera seem at first sight to be rather different. To investigate whether the model can be usefully applied to these insects, the mechanical behaviour of the wings of three species of flies, the crane fly *Tipula paludosa*, the drone fly *Eristalis tenax* and the bluebottle *Calliphora vicina* (Fig. 8), was investigated by subjecting them to a series of mechanical tests.

If the torsional model is valid, torsion of the whole wing and camber production should be dependent on torsion of the leading edge. Immobilizing the inner zones of the leading edge, zones 1 and 2 separately, should each reduce the compliance

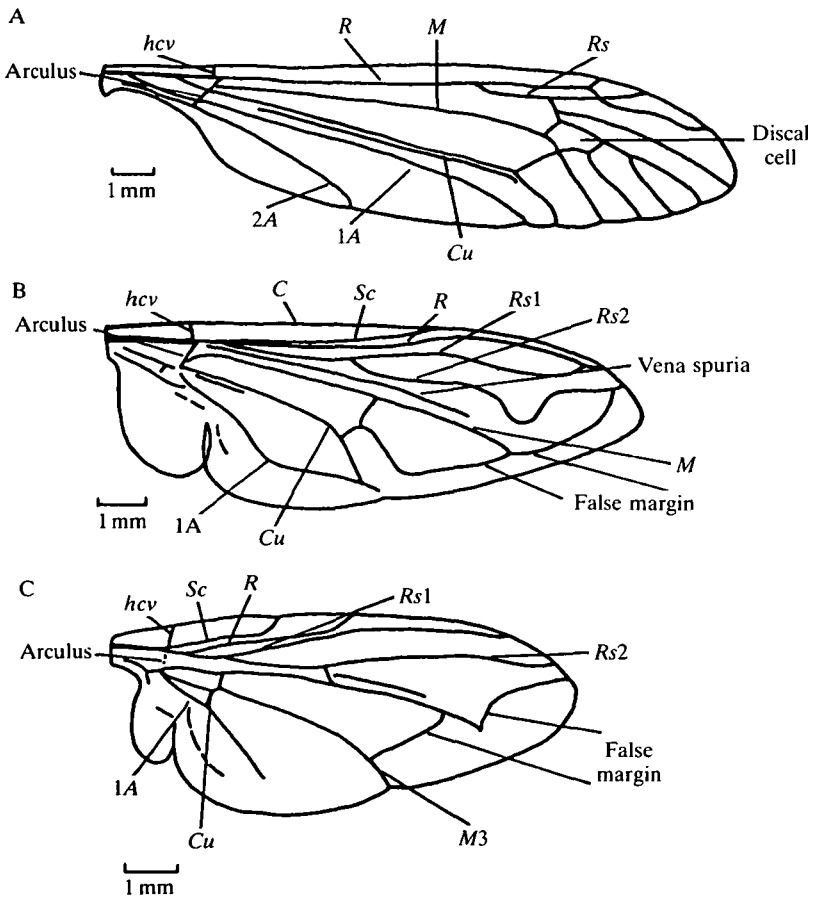

Fig. 8. The wings of (A) *Tipula paludosa*, (B) *Eristalis tenax* and (C) *Calliphora vicina*, showing the venation pattern. Each insect had a leading edge spar reinforced by the costa (*C*), sub-costa (*Sc*) and radius (*R*). In *Tipula* the main rear spars are the cubitus (*Cu*), and the two anal veins (1*A* and 2*A*); in *Eristalis*, the vena spuria and the cubitus; and in *Calliphora*, the second radial sector vein (*Rs*2) and the rear branch of the media (*M*3). The base of the cubitus is supported in all the species by a fold of cuticle, the arculus. *hcv*, humeral cross vein.

of the wing to torsion. Immobilizing zone 2 should also reduce the compliance to camber.

The premise of the wing model is that the shape changes of the wing in flight are brought about automatically. The aerodynamic forces that are generated during a wingstroke have to be strong enough to cause the wing to twist by around 10° and to set up the camber of several percent of the chord seen during each half-stroke (Nachtigall, 1966, 1981; Ellington, 1984*a*; Dudley, 1987; Ennos, in preparation). Data from mechanical tests can also verify whether the pitch changes of the whole wing, usually around 90° between strokes, caused automatically by inertial effects (Ennos, 1988), could be maintained by aerodynamic forces during each stroke.

A qualitative study of the functional morphology of the three wings (Ennos, in preparation) suggests that they most closely resembled the model wing with diverging spars. The spars (corrugations of membrane or strong reinforced wing veins) are shown in Fig. 8. The leading edge functional zones (Fig. 9) (the boundaries between them being the branching point of the first spar, between zones 1 and 2) and the branching point of the spar reaching the wingtip approximately at the trailing edge of the wing (between zones 2 and 3) were identified. In all cases both zones 1 and 2 were very short. Immobilizing only a small region of the wing base should therefore greatly reduce the compliance of the wing if the model is valid.

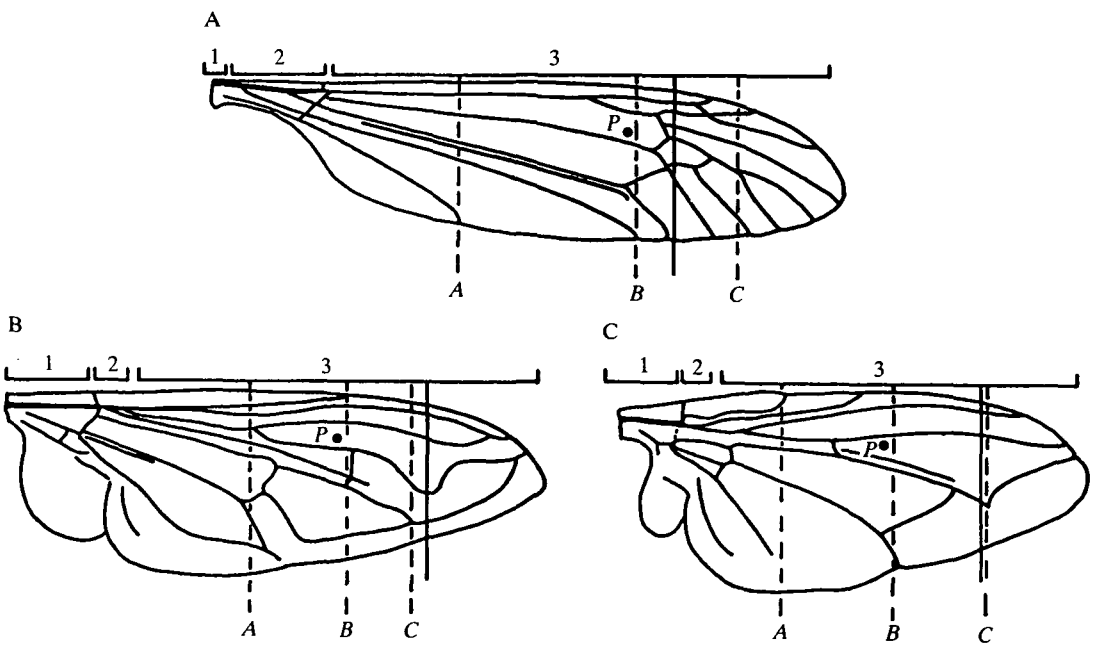

Fig. 9. The wings of (A) *Tipula paludosa*, (B) *Eristalis tenax* and (C) *Calliphora vicina* showing the estimated extent of the leading edge zones. In point force tests the force was applied at the point *P*, and the movement of the cross-sections *A*, *B* and *C* was examined. For torsion tests the tip of the wing was clamped to the pendulum rod down to the chord shown by the solid line.

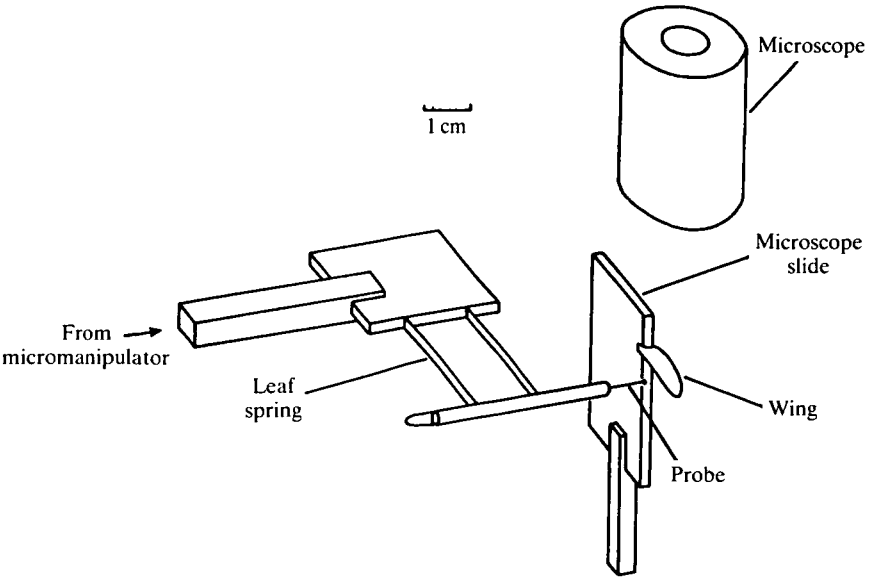

Fig. 10. The apparatus used for the point force tests.

Materials and methods

During a wingstroke, aerodynamic forces will be produced over the whole of the wing area, but the spatial and temporal distribution of these forces are both unknown (Ellington, 1984*b*). Without further knowledge of the distribution, the best that can be done is to apply discrete forces or torques to the wings. Though the loading will be rather unnatural, it can at least be of approximately the correct magnitude and will be relatively easy to apply. In this study two series of tests were performed.

Spanwise torsion and wing camber were investigated by applying a point force at the estimated centre of pressure and measuring deflections of the wing. A point application of force is the only arrangement which would not constrain the shape of the wing chord. To achieve this, however, the wing had to be removed from the body and basally clamped. The compliance of the wing articulation was therefore lost. I have suggested (Ennos, 1987) that a one-way hinge just outboard of the wing articulation, allowing supination but not pronation, may provide the compliance which allows most of the change in pitch between strokes.

In the other series of tests, wings of intact insects that had been recently killed were subjected to torsion. The effects of the articulation and wing base on torsion could therefore be measured but, since the test involved clamping the wing tip, the shape of the wing was constrained and camber could not be investigated.

Point force tests

The wing of a freshly killed insect was severed from the body as close to the wing articulation as possible and basally mounted on a microscope slide, forming a cantilever. The slide was mounted so that the wing chord was vertical (Fig. 10) and

a load was applied at the point P (this being the point estimated to be the centre of pressure, being roughly at the quarter chord and at the centre of the second moment of area from the base) (Fig. 9), using a mechanical force transducer. Two parallel strips of thin copper sheet gave a high compliance to bending of around $1\,mN^{-1}$. The transducer was advanced using a calibrated micromanipulator accurate to within 10 μm until the probe of the transducer, and therefore point P of the wing, had advanced by 0·5 mm. This distance was measured by a Zeiss stereo microscope at 40× magnification with a graduated eyepiece that gave divisions 25 μm apart. The deflection of the copper strips of the force transducer was equal to the difference between the movement of the micromanipulator and of the probe. From this the force applied could be calculated from the calibration graph of the transducer which was almost linear. The micromanipulator was returned to its original position and the wing allowed to recover. Since it was the displacement of the point P that was kept constant, the force applied at this point would obviously vary with the stiffness of the wing.

Subsequently the displacements from their rest position of several points along each of the three cross-sections of the wing A, B and C (Fig. 9) were measured when the wing was stressed by this force, again using the calibrated eyepiece. Measurements were always taken within 10 s of stressing the wing to minimize creep and the wing was allowed to return to its rest position before the next reading was taken. From these measurements the change in camber at each cross-section could be calculated as could the spanwise torsion of the wing between chords A and C.

Having measured the displacement of each of these points, the wing was either reversed and the tests repeated or a zone (1 or 2) of the leading edge was immobilized by filling up the leading edge spar with 5-min epoxy resin before repeating the tests from the same side. This would greatly increase the torsional stiffness of the leading edge at this point. In *Eristalis* and *Calliphora* glueing zone 2 involved immobilization of the arculus. Several replicates of each test were taken for each species.

The entire test was carried out in 20 min after killing the insect and the wing was surrounded by, though not in contact with, tissue pads soaked in water to reduce any water loss in the wing which would affect the properties of the cuticle. In two test runs in which tests were repeated after remounting the slide in the apparatus, there was no difference between the compliance of the two replicates, and individual readings differed by up to only 25 μm, only around 3 % of the maximum deflections.

Torsion tests

The right wing of a freshly killed insect was removed and the tip of the left wing (to the solid chordwise line shown on the wing in Fig. 9) was glued flat to an aluminium plate. When the glue had set, the plate was attached vertically along the bottom of the pendulum rod of a torque balance (Fig. 11) so that the wing chord was parallel to the rod and the leading edge of the wing followed the line of

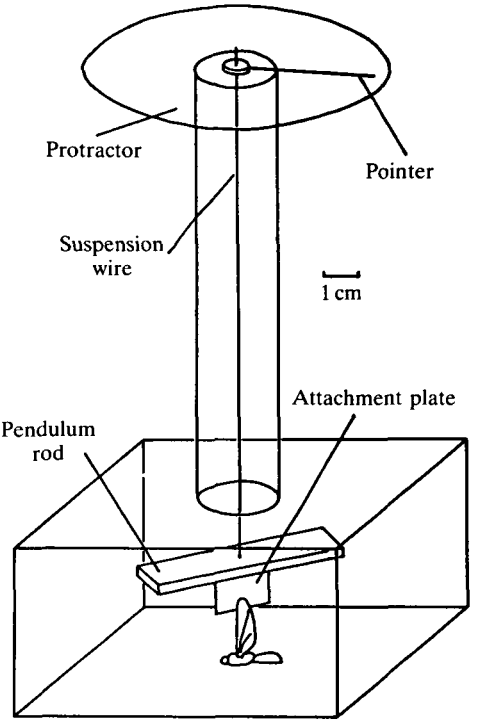

Fig. 11. The apparatus used for the torsion tests.

the torsion wire, the wing and insect's body hanging vertically. The wire was lowered until the body just touched the base of the apparatus to which it was then set by sealing wax. The outstretched wing was therefore set in its unstressed orientation. The torsional behaviour of the wing and articulation was then investigated. The top of the wire, which had a torsional compliance of around 10^6 rad Nm^{-1} was rotated in stages of 10 or 20° and the angular displacement of the pendulum rod (and hence the wing tip) was read using the protractor mounted on the apparatus. First the wing was serially supinated up to around 90°, then after returning it to rest, pronated.

Having performed this test the leading edge of the wing was then successively immobilized by filling it with 5-min epoxy resin glue (i) at the very base of the wing, (ii) up to the end of zone 1, (iii) up to the end of zone 2. The torsional behaviour of the system was taken after each of these treatments. It proved impossible to immobilize outer zones alone, due to the flow of the glue.

From these readings a graph of the restoring couple against the angular displacement of the wing could be drawn. For each insect separate values of torsional compliance for pronation and supination were calculated by linear regression of the data points each side of the unstressed orientation. Three to five insects of each species were tested.

Readings could be taken to the nearest degree. There was little creep and at the

end of the test wings returned to within 2° of their rest position. Great care was taken to prevent water loss and the atmosphere of the apparatus was kept saturated with water vapour. During the time of the experiment, up to 1 h, there was no significant variation in rigidity. There was no time to repeat readings but since the torsional compliance in pronation and supination were each found by regression of 7–15 points, the error in the calculation of compliance caused by random errors in readings must have been very low. Between insects, however, there were differences due to mounting and individual variation, so the effect of external forces on a 'typical' insect can only be found to within an order of magnitude.

Results

Point force tests

Intact wings

As the wings were pushed they both twisted along their length and developed camber in the directions predicted by the model, so that, for instance, a force from below caused pronation and dorsal arching of the wing chord. As an example the first result for *Eristalis* is shown in Fig. 12. The camber of each section was found by dividing its maximum displacement from the chord by the chord length. Torsion along the wing was estimated as the difference in pitch between sections *A* and *C*. Compliance is defined as displacement divided by applied force.

More camber tended to be produced near the pointer than elsewhere. Under natural loading the camber is likely to be more constant. Mean values of compliance to torsion and camber when forces are applied from both below and above are given for each species in Table 1, along with the standard deviation and number of insects tested. These values were used to calculate the deflections of the wings which might be expected in flight.

The forces acting on a wing during a half-stroke may be roughly estimated using the quasi-steady analysis and balance of forces for hovering flight (Weis-Fogh, 1973; Ellington, 1984*b*). The peak velocity of a wing executing simple harmonic motion is the square root of two times the average velocity. Since force is approximately proportional to the square of velocity, the peak force should reach twice the average value. The peak lift force on each wing is therefore approximately equal to the animal's weight and the resultant force at right angles to the wing will also have this value. Average values for the three species are given in Table 1 and are similar to the forces applied during the tests. The mean values of camber and torsion which should be produced in flight were calculated for each species assuming Hookean behaviour of the wings: deflections were assumed to be proportional to the forces applied. For each insect the compliance of the wing to torsion and camber was therefore multiplied by the peak aerodynamic force expected in flight. The results are given in Table 1. They show that cambers of around 10 % and spanwise torsion of around 12° should occur during the flight of *Eristalis* and *Calliphora*, and higher values during the flight of *Tipula*. There are no

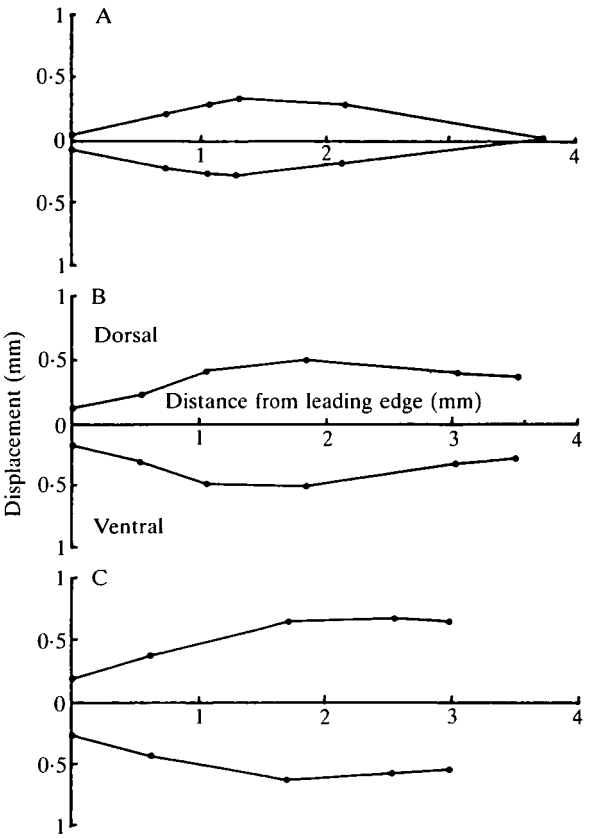

Fig. 12. Results of the point force test on an intact *Eristalis*. Dorsal movement results from a force applied from below: ventral movement from a force applied from above. From the graph camber and torsion can be readily measured. Force from below was 7×10^{-4} N. Force from above was $9{\cdot}6\times10^{-4}$ N. A, B and C show displacement of points on the three cross-sections *A*, *B* and *C*, respectively.

very reliable figures for the spanwise torsion or camber of wings in flight, the angle of attack measurements of Dudley (1987) being subject to too much error, but the values seem to be of the same order of magnitude as those estimated from films. The higher values for *Tipula* reflect the greater spanwise torsion observed in this species.

Effects of leading edge immobilization

Immobilizing the basal zones of the leading edge tended greatly to reduce the compliance of the wings, as is predicted by theory. For each insect tested the torsional compliance and ease of camber found after immobilization of the leading edge zone were divided by the values found before immobilization to give ratios of compliance after/before immobilization. The mean and standard error of these values for each species are given in Table 2 together with the number of wings

Table 1. *Behaviour of intact wings to a point force*

A *Mean compliance in torsion ($\times 10^3$ degrees N^{-1}) and camber ($\times 10^3$ % N^{-1})*

Insects	From below (downstroke) Torsion	Camber	From above (upstroke) Torsion	Camber
Tipula (4)	90·8 ± 32·8	68·0 ± 38·0	143·0 ± 71·5	86·5 ± 48·0
Calliphora (4)	19·5 ± 7·8	18·7 ± 8·0	18·2 ± 8·0	17·7 ± 7·3
Eristalis (3)	12·2 ± 3·3	9·8 ± 2·7	8·4 ± 2·2	7·8 ± 2·7

B *Approximate values of peak aerodynamic force (= average weight of an insect)*

Tipula 4×10^{-4} N	*Calliphora* 6×10^{-4} N	*Eristalis* 10^{-3} N

C *Mean expected deflection in flight*

Insect	From below (downstroke) Torsion (degrees)	Camber (%)	From above (upstroke) Torsion (degrees)	Camber (%)
Tipula	36·3 ± 13·1	27·2 ± 15·1	57·2 ± 28·6	34·6 ± 19·2
Calliphora	11·7 ± 4·7	11·2 ± 4·8	10·9 ± 4·8	10·6 ± 4·4
Eristalis	12·2 ± 3·3	9·8 ± 2·7	8·4 ± 2·2	7·8 ± 2·7

Values are means ± S.D.
Values in parentheses show the number of wings tested.

tested. The effects of immobilizing both zones 1 and 2 are given for *Eristalis* and *Calliphora*. In *Tipula* the mounting of the wing immobilized all the short zone 1 region so the results of immobilizing zone 2 alone are given for this species.

Effects on torsion. Theory predicts that immobilizing both zones 1 and 2 should reduce the torsional compliance. It can be seen that in *Eristalis* and *Calliphora* both treatments nearly halved torsional compliance, whereas in *Tipula* immobilization had an even greater effect: all results being in agreement with theory.

Effects on camber. Theory predicts that immobilizing zone 2 should reduce the compliance to cambering, whereas the same treatment with zone 1 should have no effect. The results show that immobilizing both zones reduced the compliance to camber.

Torsion tests

Rest orientation of the wing

In both *Eristalis* and *Tipula* the wing was at rest with the chord approximately parallel to the body axis. In *Calliphora* the wing was supinated about 10° from this point at rest.

Table 2. *Mean effect of zone immobilization on compliance to torsion and camber*

Insects	Zone	Compliance after/ compliance before Torsion	Camber
Calliphora (4)	1	0·52 ± 0·10	0·55 ± 0·28
Calliphora (4)	2	0·59 ± 0·12	0·46 ± 0·12
Eristalis (3)	1	0·42 ± 0·13	0·47 ± 0·10
Eristalis (3)	2	0·49 ± 0·22	0·58 ± 0·22
Tipula (1)	2	0·21	0·42 ± 0·19

Values are means ± S.D.
Values in parentheses show the number of wings tested.

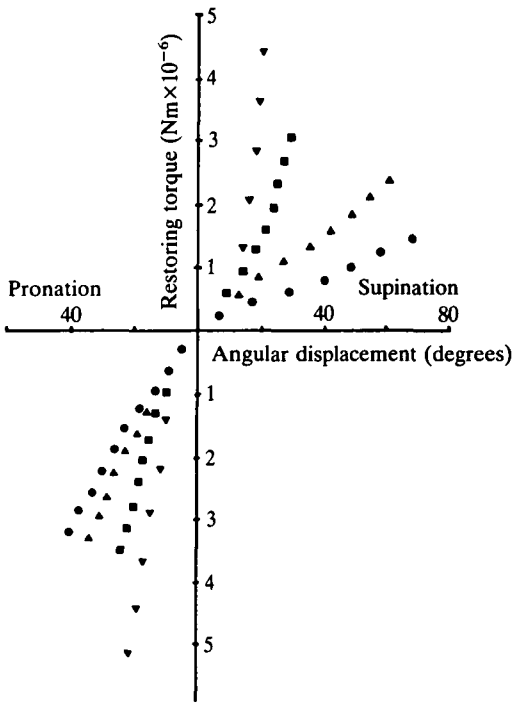

Fig. 13. Results of the torsion test on an *Eristalis*, successively immobilizing the wing base by glueing. Circles, intact wing; triangles, base glued; squares, zone 1 immobilized; inverted triangles, zones 1 and 2 immobilized.

Results of tests

The result of the first torsion test on *Eristalis* is shown in Fig. 13. Similar graphs were drawn for all insects tested and values of torsional compliance were calculated for both pronation and supination as the wing zones were progressively immobilized.

Table 3. *Behaviour of intact wings in the torsion test*

A *Mean torsional compliance* ($\times 10^6$ *degrees* Nm^{-1})

Insects	Pronation	Supination
Tipula (3)	62·3 ± 24·9	449 ± 244
Calliphora (4)	21·6 ± 5·0	59·9 ± 23·8
Eristalis (3)	11·1 ± 1·8	51·8 ± 11·9

B *Approximate peak aerodynamic torques*

Tipula 2×10^{-7} Nm	*Calliphora* 3×10^{-7} Nm	*Eristalis* 5×10^{-7} Nm

C *Mean calculated changes in angle of attack in flight*

Insect	Pronation (degrees)	Supination (degrees)
Tipula	12·5 ± 4·6	89·8 ± 48·8
Calliphora	6·4 ± 1·5	17·7 ± 7·1
Eristalis	5·6 ± 0·9	25·9 ± 6·0

Values are means ± S.D.
Values in parentheses show the number of wings tested.

Intact insects. Mean values for the torsional compliance of the three species are given in Table 3 with the standard deviation and the numbers of insects tested. In all cases the torsional compliance in supination was far greater than in pronation. Thus a given torque should cause a greater degree of supination.

The torque around the torsional axis of the wing equals the aerodynamic force multiplied by the perpendicular distance of the centre of the force from the torsional axis. Using the estimates of peak aerodynamic forces given in Table 2 and assuming that the centre of pressure is at the quarter chord, 1 mm from the leading edge and around 0·5 mm behind the axis of torsion (Ennos, 1988), it is therefore possible to estimate the torque applied to a wing during a stroke. Estimated torques are given in Table 3.

The mean resulting rotation of the wing that would be caused by these torques in each of the insects tested was calculated, again assuming Hookean behaviour, by multiplying the torsional compliance by the torque applied. The mean values expected for each species are given in the table. It can be seen that aerodynamic torque can supinate the wing substantially, especially in *Tipula*, but is only capable of pronating the wing by a few degrees.

Effect of immobilizing basal leading edge zones

The ratios of torsional compliance before and after immobilization of basal zones were calculated and mean values are given for each species in Table 4. It can be seen that in each case successive immobilization reduced torsional compliance.

Effect of immobilizing the wing base. The effect of immobilizing the very base of the wing was greatly to reduce the torsional compliance in supination, whereas the compliance in pronation was only slightly reduced. The effect is less pronounced in *Calliphora* than in the other species. This result is in agreement with the hypothesis (Ennos, 1987) that most of the torsional compliance of the wing resides in a one-way hinge at the base of the radius.

Effect of immobilizing zones 1 and 2. Immobilizing the rest of zone 1 further reduced the compliance of the system in agreement with theory. Immobilizing zone 2 reduced compliance still further. According to the model this should remove *all* compliance. The model, however, assumes that wing spars are effectively rigid in bending. Under the stresses applied in this case by the apparatus the wing veins buckled and bent in a manner not seen in flight. Some compliance, therefore, remained.

Discussion

Wing structure

The behaviour of the wings agreed well with that predicted by the torsional model. Upon application of a force behind the leading edge the wings twisted along their length and camber was produced in the direction predicted by the model. The longitudinal veins remained straight and distortion was effected by the torsion of the veins. Immobilizing merely the first 15–20 % of the leading edge reduced the torsional compliance in the torsion tests by an average of around 75 %.

The model predicts that compliance to camber will be reduced by immobilizing zone 2 but be unaffected by similar treatment of zone 1. The results show that immobilizing zone 2 did indeed reduce camber, but so did immobilizing zone 1 in *Eristalis* and *Calliphora*. This departure from the model may be due to the connections between the cubitus and the first anal vein (1*A*) described in Ennos (in preparation). Immobilizing 1*A* prevents the cubitus from rotating, so reducing the camber formed in the wing.

Table 4. *Mean effects of successive leading edge immobilization on torsional compliance of wings*

	Compliance after immobilization/compliance of intact wing					
	Pronation			Supination		
Insects	Base	Zone 1	Zone 2	Base	Zone 1	Zone 2
Tipula (3)	0·90 ± 0·07		0·46 ± 0·01	0·46 ± 0·29		0·08 ± 0·05
Calliphora (4)	0·81 ± 0·08	0·59 ± 0·06	0·33 ± 0·13	0·69 ± 0·25	0·43 ± 0·17	0·22 ± 0·05
Eristalis (3)	0·84 ± 0·04	0·47 ± 0·02	0·30 ± 0·06	0·46 ± 0·17	0·15 ± 0·08	0·07 ± 0·02

Values are means ± S.D.
Values in parentheses show the number of wings tested.

The crudity of the tests and the difficulty of accurately immobilizing specific zones prevented any meaningful comparisons of the venation of the species.

Response to aerodynamic forces

It is clear that the forces occurring in flight are of the right order of magnitude to produce the degree of spanwise torsion and camber seen in the films of insects in free flight. Point force tests suggested an equal compliance to torsion and camber in both pronation and supination. The torsion tests on intact insects, however, showed that the base of the wing allows supination but not pronation. As a result, the torques produced during the downstroke would be sufficient to pronate the wing only a few degrees from the rest position nearly parallel to the body axis. This is the orientation seen in the free-flight films. Appreciable torsion would be caused during the upstroke, calculated values ranging from 17° in *Calliphora* to 25° in *Eristalis* and 90° in *Tipula*. These torques will help keep the wing in its supinated state after the inertia of the wing has caused the wing to rotate at lower stroke reversal (Ennos, 1988).

The evidence from these tests and from Ennos (1988) confirms that the basic changes in wing shape and orientation may be effected by the aerodynamic and inertial forces which result from the motion of the wing.

Conclusion

There seem to be good reasons why insect wings are not constructed like the wings of modern aircraft. The monocoque structure of aircraft wings strongly resists torsion. The wings of insects, however, have to twist between wingbeats to optimize the performance of the aerofoil. The open, corrugated structure of the wings of many insects, in which spars branch serially from the leading edge, allows such torsion and causes camber to be set up automatically as the wing is twisted. The exact pattern of deformation is determined by the orientation and shape of the wing spars. Such wings also allow controlled yield upon impact loading (Newman & Wootton, 1986).

The resulting wing seems to be a perfectly designed automatically adjusting aerofoil, responding to the forces encountered in flight with shape changes that improve its efficiency.

Insect wings are not the only structures to which the model may be applicable, since camber can be automatically produced by any structure in which spars branch from a leading edge that is subject to twisting or rotation. The primary feathers of birds diverge from the leading edge of the wing in just such a manner. In birds whose wings undergo large angles of rotation, such as hummingbirds, torsion of the leading edge (largely at the joints) may cause camber to be formed.

Recent evidence (Padian, 1988) also shows that the wing membrane of pterodactyls was supported by spars of keratin branching from the leading edge and orientated in a manner similar to the feathers of birds. It is tempting to suggest that the proposed mechanism for camber production may also have been used by these creatures.

I thank Dr R. J. Wootton for his help and criticism during this work and in production of the manuscript. The work was carried out under tenure of an SERC research studentship.

References

DUDLEY, T. R. (1987). The mechanics of forward flight in Insects. Ph.D. thesis, University of Cambridge.

ELLINGTON, C. P. (1984*a*). The aerodynamics of hovering insect flight. III. Kinematics. *Phil. Trans. R. Soc. Ser.* B **305**, 41–78.

ELLINGTON, C. P. (1984*b*). The aerodynamics of hovering insect flight. VI. Lift and power requirements. *Phil. Trans. R. Soc. Ser.* B **305**, 145–181.

ENNOS, A. R. (1987). A comparative study of the flight mechanism of Diptera. *J. exp. Biol.* **127**, 355–372.

ENNOS, A. R. (1988). The inertial cause of stroke reversal in Diptera. *J. exp. Biol.* **140**, 161–169.

GORDON, J. E. (1978). *Structures or Why Things Don't Fall Down.* Penguin Books.

HERTEL, H. (1966). *Structure, Form, Movement.* New York: Reinhold.

NACHTIGALL, W. (1966). Die Kinematik der Schlagflügelbewegungen von Dipteren. Methodische und Analytische Grundlagen zur Biophysik des Insektenflugs. *Z. vergl. Physiol.* **52**, 155–211.

NACHTIGALL, W. (1981). Insect flight aerodynamics. In *Locomotion and Energetics in Arthropods* (ed. C. F. Herreid & C. R. Fourtner), pp. 127–162. New York: Plenum Press.

NEWMAN, B. G., SAVAGE, S. B. & SCHOUELLA, D. (1977). Model tests on a wing section of an *Aeschne* dragonfly. In *Scale Effects in Animal Locomotion* (ed. T. J. Pedley), pp. 445–477. London: Academic Press.

NEWMAN, D. J. S. (1982). The functional wing morphology of some Odonata. Ph.D. thesis, University of Exeter. 281pp.

NEWMAN, D. J. S. & WOOTTON, R. J. (1986). An approach to the mechanics of pleating in dragonfly wings. *J. exp. Biol.* **125**, 361–372.

NORBERG, R. Å. (1972). The pterostigma of insect wings: an inertial regulator of wing pitch. *J. comp. Physiol.* **81**, 9–22.

PADIAN, K. (1988). Pterosaurs: functional birds or functional bats? In *Biomechanics in Evolution.* S.E.B. Seminar series (in press).

REES, C. J. C. (1975*a*). Form and function in corrugated insect wings. *Nature, Lond.* **256**, 200–203.

REES, C. J. C. (1975*b*). Aerodynamic properties of an insect wing section and a smooth aerofoil compared. *Nature, Lond.* **258**, 141–142.

VOGEL, S. (1967). Flight in *Drosophila*. III. Aerodynamic characteristics of fly wings and wing models. *J. exp. Biol.* **46**, 431–443.

WEIS-FOGH, T. (1973). Quick estimates of flight fitness in hovering animals, including novel mechanisms for lift production. *J. exp. Biol.* **59**, 169–230.

WOOTTON, R. J. (1981). Support and deformability in insect wings. *J. Zool., Lond.* **193**, 447–468.